Applied Physics B (2022) 128:11
https://doi.org/10.1007/s00340-021-07730-6

Applied Physics B
Lasers and Optics

Quantum coherence in electrically pumped organic interferometric emitters

F. J. Duarte[1,2] · **T. S. Taylor**[3]

Received: 4 April 2021 / Accepted: 9 December 2021 / Published online: 29 December 2021

Abstract
Electrically pumped organic semiconductors have been demonstrated to yield nearly diffraction-limited beam divergences and high-visibility double-slit interferograms characteristic of laser emission. This coherent emission has been measured and quantified in detail but no explanation has been advanced on the origin of this emission. Here, the origin of this emission is explained in terms of probability amplitudes *à la Dirac*. More specifically, in terms of Dirac's identities applicable to quanta "absolutely indistinguishable from one another." In addition, this elucidation enables the cohesive understanding of sources applicable to quantum entanglement experiments.

1 Introduction

Coherent emission from electrically pumped organic semiconductors was reported by Duarte et al. [1] while utilizing a coumarin 545 tetramethyl laser dye-doped tandem organic light-emitting diode (OLED) electrically excited in the pulsed regime with nanosecond rise time pulses.

This coherence is characterized by highly directional emission, with a near diffraction-limited beam at $\Delta\theta \approx 2.53$ mrad, and high visibility interferometric fringes with $\mathcal{V} \approx 0.9$ [1–3]. Albeit these results have been analyzed and quantified in detail [4] to date the origin of this coherent emission has not been elucidated. This is done here from a quantum mechanical perspective.

Furthermore, the conceptual framework utilized in this analysis is also applied to what is known about type II spontaneous parametric down conversion (SPDC).

2 Coherent interferometric emitters: experimental

In this section, for the benefit of the reader and the sake of completeness, the experimental results disclosed in [1] are briefly reviewed. Coherent emission from an electrically excited laser dye-doped organic semiconductor was characterized in mainly two ways: directionality of the emission and the high visibility of the interference fringes of the emission. The gain medium was the high-gain laser dye coumarin 545 tetramethyl [5]. The semiconductor gain medium and the electrical excitation methodology are described in detail in [4, 6].

A detailed experimental description of the integrated interferometric device, powered by the pulsed electrically pumped organic semiconductor utilized in these measurements, and detection techniques, is given in [1–3].

A highly directional emission beam was recorded permanently on black and white silver-halide film as depicted in Fig. 1. This directional emission was measured to exhibit a beam divergence of $\Delta\theta \approx 2.53 \pm 0.13$ mrad which translates into $\Delta\theta \approx 1.09(\lambda/\pi w)$, where $(\lambda/\pi w)$ is the diffraction-limited beam divergence and $\lambda \approx 540$ nm. The digital beam profile of this emission is near-Gaussian [1]. This class of beam profile and measured beam divergence is typical of optimized narrow-linewidth laser oscillator emission [7].

Figure 2 shows the digital image of the profile of the double-slit interferogram of the highly directional on-axis emission from the electrically pumped laser-dye doped organic semiconductor emitter. The width of the slits was 50 μm and

✉ F. J. Duarte
francisco.duarte@uah.edu

[1] Interferometric Optics, Jonesborough, TN, USA

[2] University of Alabama in Huntsville, Alabama, USA

[3] US Army Space and Missile Defense Command, Huntsville, AL, USA

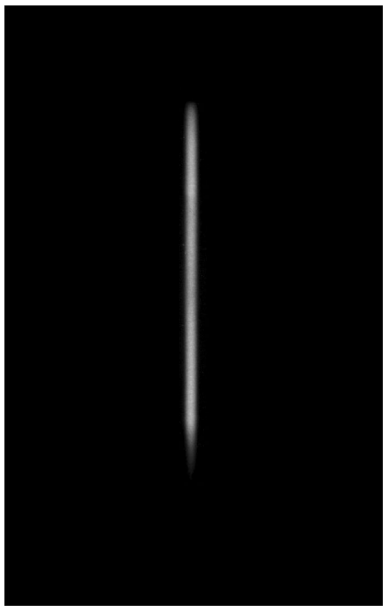

Fig. 1 Silver halide photographic image of the cross section of the on-axis emission from the electrically pumped laser-dye doped organic semiconductor (from [1])

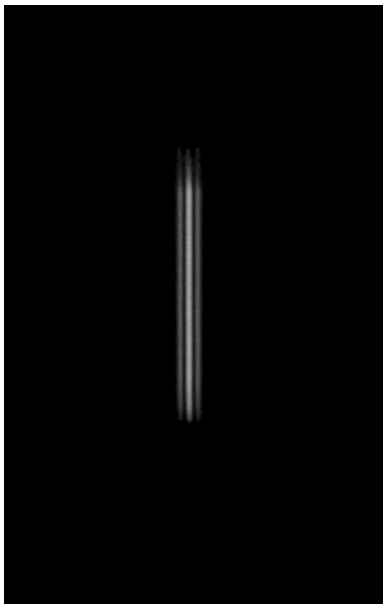

Fig. 3 Silver halide photographic image of the double-slit interferogram of the highly directional on-axis emission from the electrically pumped laser-dye doped organic semiconductor emitter (from [1])

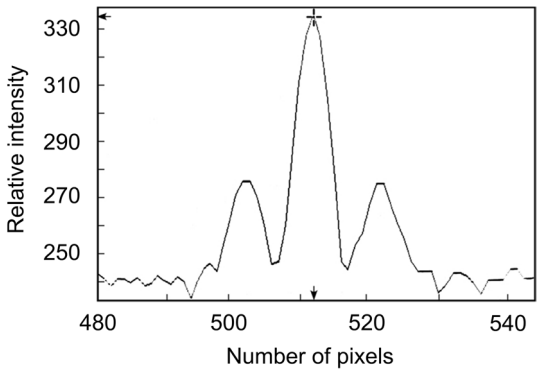

Fig. 2 Digital image of the double-slit interferogram of the highly directional on-axis emission from the electrically pumped laser-dye doped organic semiconductor emitter. On the x axis each pixel is 25 μm wide (from [1])

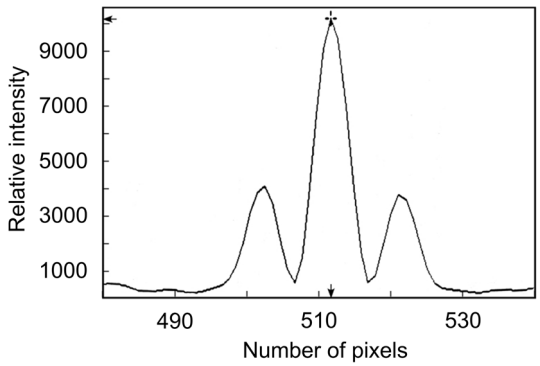

Fig. 4 Digital image of the double-slit interferogram of the highly directional on-axis emission from the $(3s_2 - 2p_{10})$ transition of a He–Ne laser emission under an identical interferometric configuration. On the x axis each pixel is 25 μm wide (from [1])

the slits were also separated by 50 μm. Using Michelson's definition for double-slit interference visibility [8, 9] the measured visibility of this emission is $\mathcal{V} \approx 0.901 \pm 0.088$. The black and white photographic version of Fig. 2 is shown in Fig. 3.

$$\mathcal{V} = \frac{I_{\max} - I_{\min}}{I_{\max} + I_{\min}}. \tag{1}$$

Figure 4 shows the digital image of the profile of the double-slit interferogram of the highly directional on-axis emission from the $(3s_2 - 2p_{10})$ transition of a He–Ne laser, at $\lambda = 543.30$ nm, emission under an identical interferometric configuration. The interferometric configuration is identical to that utilized to record the results displayed in Fig. 2. The measured visibility of this emission is $\mathcal{V} \approx 0.952 \pm 0.031$ [2].

From an energetic perspective it should be mentioned that the interferograms captured digitally, as depicted in Fig. 2, and in silver-halide media, as shown in Fig. 3, correspond to emission in the nano Watt (nW) regime [1, 2]. In this regard, the high black-and-white contrast of the silver-halide image (Fig. 3) highlights the presence of very low levels of optical noise, or amplified spontaneous emission, in the

interferograms. Most of the noise observed in the background of Fig. 2 can be attributed to the electronic noise of the room temperature CCD detector. The combined detector noise, and optical noise, from the digital interferogram can be estimated to correspond, on average, to less than ~ 7% of the peak signal. The observed coherent emission is linearly polarized, however, explicit polarization measurements were not performed.

3 Coherence

The emission measurements presented in the previous section are characterized by a nearly diffraction-limited beam divergence $\Delta\theta \approx 1.09(\lambda/\pi w)$, with a near-Gaussian beam profile, and an interferometric visibility of $\mathcal{V} \approx 0.901 \pm 0.088$. These measurements point unequivocally toward strong spatial and spectral coherence characteristic of laser emission.

Is there an explanation for the spatial coherence from a classical perspective? Collett-Wolf sources are partially coherent sources known to produce Gaussian-like beams that are also directional [10]. However, there is no record in the published literature of Collett-Wolf sources yielding interferometric visibilities in the laser range, that is, in the $0.85 \leq \mathcal{V} \leq 1.0$ range. Therefore a Collett–Wolf type phenomena must be discarded as a possible explanation.

It should be noted that in the published literature, emission associated with interferometric visibilities in the range $0.85 \leq \mathcal{V} \leq 1.0$ is considered as laser emission [11–15]. By contrast, semi-coherent and non-laser sources including standard $Alql_3$ OLED devices, and amplified spontaneous emission sources, yield interferometric visibilities typically in the range of $0.40 \leq \mathcal{V} \leq 0.65$ [16–18].

Since the gain medium length is $L \approx 300$ nm, and emission wavelength $\lambda \approx 540$ nm, the cavity is really a sub-microcavity, or nanocavity, operating in the $L \leq \lambda$ regime where laser thresholds decrease dramatically. Indeed, De Martini [19] reports on a near "zero-threshold-laser" for a cavity length of $L \approx \lambda/2$. This observation was made while experimenting on a multiple-transverse-mode optically pumped dye laser [19]. One subtle aspect of sub-microcavities is that the emission can be single-longitudinal-mode albeit the laser linewidth might not necessarily be as narrow as that emitted from macroscopic laser cavities [7]. This is due to one of the consequences of Heisenberg's uncertainty principle $\Delta p \Delta x \approx h$ which leads to $\Delta\lambda \approx \lambda^2/\Delta x$, where Δx is related to the cavity length.

Assuming perfect and intrinsic coherent illumination either from a single photon or an ensemble of indistinguishable photons the interferometric spatial distribution can be calculated from the Dirac–Feynman principle [20, 21]

$$\langle d|s\rangle = \sum_{j=1}^{N} \langle d|j\rangle \, \langle j|s\rangle, \tag{2}$$

where s is the photon source and d is the detector or interferometric plane. The index j refers to the jth slit in the N-slit array ($j = 1, 2, 3...N$) [22, 23]. Multiplication of (2) with its complex conjugate yields the interferometric probability [22]

$$\langle d|s\rangle\langle d|s\rangle^* = \left(\sum_{j=1}^{N} \langle d|j\rangle \, \langle j|s\rangle\right)\left(\sum_{j=1}^{N} \langle d|j\rangle \, \langle j|s\rangle\right)^*, \tag{3}$$

$$|\langle d|s\rangle|^2 = \sum_{j=1}^{N} \Psi(r_j) \sum_{m=1}^{N} \Psi(r_m) e^{i(\Omega_m - \Omega_j)}, \tag{4}$$

and using the exponential identity

$$2\cos(\Omega_m - \Omega_j) = e^{-i(\Omega_m - \Omega_j)} + e^{i(\Omega_m - \Omega_j)}, \tag{5}$$

(4) can be expressed as the series [22, 23]

$$|\langle x|s\rangle|^2 = \sum_{j=1}^{N} \Psi(r_j)^2 + 2\sum_{j=1}^{N} \Psi(r_j)\left(\sum_{m=j+1}^{N} \Psi(r_m)\cos(\Omega_m - \Omega_j)\right). \tag{6}$$

These three equivalent equations lead to a diffraction-limited beam divergence [23] and can be classified as representing l_2 norm coherence [24]. It is also relevant that recently it has been indicated that the inherent coherence is related to the visibility $\mathcal{V}$ of the fringes [25, 26]. Further relevant discussions on coherence from a quantum perspective are given in [27, 28].

The interferogram thus calculated is displayed in Fig. 5. In this theoretical interferogram the separation of the two secondary peaks is $\Delta d \approx 490$ µm which should be compared to $\Delta d \approx 484$ µm from the measured interferogram depicted in Fig. 2 and $\Delta d \approx 485$ µm from the measured interferogram depicted in Fig. 4.

4 The quantum perspective

As highlighted in previous publications [29–31], crucial to the derivation of the quantum entanglement probability amplitude [32, 33]

$$|\psi\rangle = 2^{-1/2}(|x\rangle_1|y\rangle_2 \pm |y\rangle_1|x\rangle_2), \tag{7}$$

via the Dirac–Feynman interferometric principle [20, 21]

$$\langle d|s\rangle = \sum_{j=1}^{N} \langle d|j\rangle \, \langle j|s\rangle$$

is the Dirac identity [20]

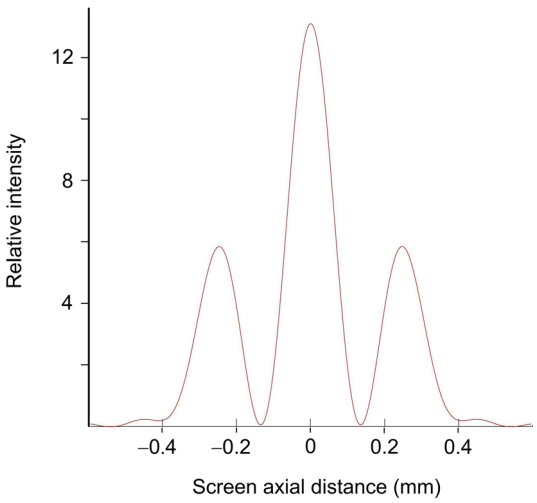

Fig. 5 Calculated profile of the double-slit interferogram. Here, $N = 2$, slit width and slit separation is 50 μm, $\lambda = 540$ nm, and the intra interferometric distance is $D_{\langle d|j\rangle} = 50$ mm

$$|X\rangle = |a\rangle_1|b\rangle_2|c\rangle_3...|g\rangle_n, \tag{8}$$

which means that indistinguishable quanta 1, 2, 3, … n can be in different states. When referring to this "curious phenomena… having no analogue in classical theory" Dirac is writing about quanta of the "same kind" and "absolutely indistinguishable from one another" [20]. At the same time, he is also contemplating arrays of identical quanta in different sates such as $|a\rangle_1, |b\rangle_1, |c\rangle_1...$ and $|a\rangle_2, |b\rangle_2, |c\rangle_2....$ It is then natural to extend the Dirac identity $|X\rangle = |a\rangle_1|b\rangle_2|c\rangle_3...|g\rangle_n$ to

$$|Y\rangle = |a\rangle_1|b\rangle_1|c\rangle_1...|g\rangle_1, \tag{9}$$

and

$$|Z\rangle = |a\rangle_2|b\rangle_2|c\rangle_2...|g\rangle_2, \tag{10}$$

and so on, that apply to the very same, utterly indistinguishable, quanta in different states.

This leads to the concept of a series of indistinguishable quanta in different states of polarization [31]. In general, Dirac tabulates the various possible series of states in the determinant

$$\begin{vmatrix} |a\rangle_1 & |a\rangle_2 & |a\rangle_3 & \cdots & |a\rangle_n \\ |b\rangle_1 & |b\rangle_2 & |b\rangle_3 & \cdots & |b\rangle_n \\ |c\rangle_1 & |c\rangle_3 & |c\rangle_3 & \cdots & |c\rangle_n \\ \cdot & \cdot & \cdot & \cdots & \cdot \\ \cdot & \cdot & \cdot & \cdots & \cdot \\ \cdot & \cdot & \cdot & \cdots & \cdot \\ |g\rangle_1 & |g\rangle_2 & |g\rangle_3 & \cdots & |g\rangle_n \end{vmatrix}. \tag{11}$$

In this regard, more specifically, these Dirac identities are applicable, for instance, to describe single-transverse-mode single-longitudinal-mode coherent emission of indistinguishable quanta including both, $|x\rangle$ and $|y\rangle$, states of polarization.

More specifically, for $|x\rangle$ polarization, one can have

$$|\alpha\rangle = |x\rangle_1|x\rangle_2|x\rangle_3...|x\rangle_n, \tag{12}$$

and for $|y\rangle$ polarization

$$|\beta\rangle = |y\rangle_1|y\rangle_2|y\rangle_3...|y\rangle_n. \tag{13}$$

These identities describe precisely and elegantly what coherent emission is at its most fundamental level: ensembles of indistinguishable quanta in a given state of polarization.

In an interferometric emitter, with minimized optical noise, the emission is comprised of highly indistinguishable quanta giving rise to high-visibility interference as demonstrated in Fig. 2.

5 The quantum perspective on spontaneous parametric down conversion

Spontaneous parametric down-conversion (SPDC) sources [34, 35] yield photon pairs with entangled polarizations and as such have become widely used in quantum entanglement experiments.

For type I SPDC it is said [34] that the photon pair is correlated, as explained by Friberg [36], and that two photons in the same state of polarization and traveling in different directions are produced. The entanglement of $|R\rangle$ and $|L\rangle$ polarizations is induced via external optics [34].

For type II SPDC it is said that ordinarily polarized photons and extraordinarily polarized photons are emitted in two cones, in divergent directions, and where the two cones intersect the entangled state can be described by the superposition [35]:

$$|\psi\rangle = 2^{-1/2}(|x\rangle_1|y\rangle_2 + e^{i\alpha}|y\rangle_1|x\rangle_2). \tag{14}$$

If the value of α is set by external optics so that $e^{i\alpha} = 1$ then (14) reduces to one of the four standard probability amplitudes for quantum entanglement [31]:

$$|\psi\rangle = 2^{-1/2}(|x\rangle_1|y\rangle_2 + |y\rangle_1|x\rangle_2). \tag{15}$$

From a Diracian perspective an explanation for this entangled emission can be given as follows: one emission cone yields photon 1 polarized in the $|x\rangle$ state, and its complete description is given by $|x\rangle_1$. The other emission cone yields photon 2 polarized in the $|y\rangle$ state, and its complete description is given by $|y\rangle_2$. The geometrical interaction of the two cones allows for the assembled state

$$|A\rangle = |x\rangle_1 |y\rangle_2, \tag{16}$$

to be formed. It follows that the alternative assembled state is configured as

$$|B\rangle = |y\rangle_1 |x\rangle_2. \tag{17}$$

Hence, the complete normalized probability amplitude can be written as (15).

Here, it should be emphasized that superposition probability amplitudes of the form:

$$|\psi\rangle = |A\rangle + |B\rangle, \tag{18}$$

are intrinsic to quantum interference configurations [22, 29–31, 37].

For completeness, it should be mentioned that quantum coherence in type II SPDC has also been discussed, from different perspectives, by Menzel et al. [38] and Bolduc et al. [39].

6 On laser emission

As indicated in [4] albeit there was absolutely no doubt of the high coherence observed in [1] no claim of traditional lasing was made. Strictly speaking, claims of traditional laser emission require demonstration of mirror alignment dependence which was not possible given the experimental configuration utilized in [1]. Post 2005 there have been a number of claims of "lasing" from electrically pumped organic semiconductors. As explained in 2018 by Duarte and Vaeth [4] none of these publications demonstrate mirror alignment dependence and have been vague, and/or unclear, on key elements. More recently, however, Sandanayaka et al. [40] have reported emission characteristics compatible with those of standard broadband lasing in an electrically pumped thin film OLED device incorporating a mixed-order distributed feedback grating.

The coherent emission from the interferometric emitter discussed here is indistinguishable, as characterized by near diffraction limited $\Delta\theta$ and high $\mathcal{V}$ of the interferograms, from laser emission except for the high intensity, or high brightness, normally associated with laser emission. In lasing, an enormous population of indistinguishable quanta participates in the emission [30]. In addition, from a systems perspective, in addition to high brightness, orthodox narrow-linewidth lasers exhibit strong mirror alignment dependence [7, 23].

7 Discussion

Duarte and Vaeth [4] provide a detailed discussion describing the spatial and spectral coherence observed and succinctly summarized by the quantities $\Delta\theta \approx 1.09(\lambda/\pi w)$ and $\mathcal{V} \approx 0.901 \pm 0.088$. What had not been explained, up to now, is the origin of this emission. In other words: what is the physics that sustains this remarkable coherence, in the nW regime, at its most fundamental level? Here, it should be noted that experienced authors such as Samuel and colleagues [41, 42] did attempt to explain this coherence proposing a generic "spatial filtering" effect. However, the physics is perfectly explained via the application of (4): this generalized interferometric equation also describes diffraction via a single slit by treating the slit as being composed of hundreds of imaginary sub-slits [22, 30]. Introduction of an appropriate slit, transverse to the propagation axis, reduces the transverse-mode emission to a single-transverse-mode which, given the sub-microcavity length ($L \leq \lambda$), allows only single-longitudinal-mode emission due to the enormous intracavity mode spacing ($\lambda^2/2L \approx 486$ nm) [4]. As pointed out by Duarte and Vaeth [4], "the coherent emission is intrinsically present and the interferometric configuration's only function is to reveal it".

In an interferometric emitter, the emission is comprised of highly indistinguishable quanta giving rise to interference characterized by high visibility as demonstrated in Fig. 2. The origin of this coherence is the same Diracian physics that allows quantum entanglement to occur from an interferometric perspective. In quantum entanglement, we deal with Diracian states like $|X\rangle = |a\rangle_1 |b\rangle_2 |c\rangle_3 ... |g\rangle_n$ while in highly coherent emission we deal with ensemble states like $|\alpha\rangle = |x\rangle_1 |x\rangle_2 |x\rangle_3 ... |x\rangle_n$ which mean that all available quanta are indistinguishable and in the same state of polarization. In other words, the key role of the interferometric configuration is to allow us to detect and measure the fundamental quanta ensemble $|\alpha\rangle = |x\rangle_1 |x\rangle_2 |x\rangle_3 ... |x\rangle_n$. This ensemble of indistinguishable quanta in the same quantum state is the essence of coherent emission and/or laser emission.

Furthermore, we have outlined the physics behind type II SPDC leading to the emission of quantum entanglement states of the $|\psi\rangle = (|x\rangle_1 |y\rangle_2 \pm |y\rangle_1 |x\rangle_2)$ kind. To our knowledge this is the first time that these concepts are disclosed in the open literature.

Acknowledgements Fruitful discussions with Dr. K. M. Vaeth are gratefully acknowledged.

References

1. F.J. Duarte, L.S. Liao, K.M. Vaeth, Opt. Lett. **30**, 3072 (2005)
2. F.J. Duarte, Opt. Lett. **32**, 412 (2007)
3. F.J. Duarte, Appl. Phys. B **90**, 101 (2008)
4. F. J. Duarte, K.M. Vaeth, in *Organic Lasers and Organic Photonics*, ed. by F.J. Duarte (Institute of Physics, Bristol, 2018) **(Chapter 11)**
5. F.J. Duarte, L.S. Liao, K.M. Vaeth, A.M. Miller, J. Opt. A Pure Appl. Opt. **8**, 172 (2006)
6. F.J. Duarte, K.M. Vaeth, L.S. Liao, U S Patent 7667391 B2 (2010)
7. F.J. Duarte, Appl. Opt. **38**, 6347 (1999)

8. A.A. Michelson, *Studies in Optics* (The University of Chicago, Chicago, 1927)
9. M. Born, E. Wolf, *Principles of Optics* (Pergamon, New York, 1975)
10. E. Collett, E. Wolf, Opt. Lett. **2**, 27 (1978)
11. G.M. Shimkaveg, M.R. Carter, R.S. Walling, J.M. Ticehurst, J.A. Koch, S. Mrowka, J.E. Trebes, B.J. MacGowan, L.B. Da Silva, D.L. Mathews, R.A. London, R.E. Stewart, in *Proceedings of International Conference on Lasers' 91*, ed. by F.J. Duarte, D.J. Harris (STS, McLean, VA, 1992), pp. 84–92
12. J.E. Trebes, K.A. Nugent, S. Mrowka, R.A. London, T.W. Barbee, M.R. Carter, J.A. Koch, B.J. MacGowan, D.L. Matthews, L.B. Da Silva, G.F. Stone, M.D. Feit, Phys. Rev. Lett. **68**, 588 (1992)
13. T. Ditmire, E.T. Gumbrell, R.A. Smith, J.W.G. Tisch, D.D. Meyerhofer, M.H.R. Hutchison, Phys. Rev. Lett. **77**, 4756 (1996)
14. Y. Liu, M. Seminario, F.G. Tomasel, C. Chang, J.J. Rocca, D.T. Atwood, Phys. Rev. A **63**, 033802 (2001)
15. A. Lucianetti, K.A. Janulewicz, R. Kroemer, G. Priebe, J. Tümmler, W. Sandner, P.V. Nickless, V.I. Redkorechev, Opt. Lett. **29**, 881 (2004)
16. B.J. Thompson, E. Wolf, J. Opt. Soc. Am. **47**, 895 (1957)
17. K. Saxena, D.S. Mehta, R. Srivastava, M.N. Kamalasanan, Appl. Phys. Lett. **89**, 061124 (2006)
18. J.A. Dharmadhikari, A.K. Dharmadhikari, G.R. Kumar, Opt. Lett. **30**, 765 (2005)
19. F. De Martini, J.R. Jakobovitz, Phys. Rev. Lett. **60**, 1711 (1988)
20. P.A.M. Dirac, *The Principles of Quantum Mechanics* (Oxford University, Oxford, 1958)
21. R.P. Feynman, R.B. Leighton, M. Sands, *The Feynman Lectures on Physics* (Addison-Wesley, Reading, 1965), Vol. III
22. F.J. Duarte, Opt. Commun. **103**, 8 (1993)
23. F.J. Duarte, *Tunable Laser Optics* (Elsevier-Academic, New York, 2003)
24. T. Baumgratz, M. Cramer, M.B. Plenio, Phys. Rev. Lett. **113**, 140401 (2014)
25. N.M. Bera, T. Qureshi, M.A. Siddiqui, A.K. Pati, Phys. Rev. A **92**, 012118 (2015)
26. G. Sharma, M.A. Siddiqui, S. Mal, S.K. Sazim, A. Sen, Phys. Lett. A **384**, 126297 (2020)
27. O. Kfir, V. Di Giulio, F.J. García de Abajo, C. Ropers, Sci. Adv. **7**, abf6380 (2021)
28. A. Karnieli, N. Rivera, A. Arie, I. Kaminer, Sci. Adv. **7**, abf8096 (2021)
29. F.J. Duarte, J. Mod. Opt. **60**, 1585 (2013)
30. F.J. Duarte, *Quantum Optics for Engineers* (CRC, New York, 2014)
31. F.J. Duarte, *Fundamentals of Quantum Entanglement* (Institute of Physics, Bristol, 2019)
32. M.L.H. Pryce, J.C. Ward, Nature **160**, 435 (1947)
33. J.C. Ward, *Some Properties of the Elementary Particles* (Oxford University, Oxford, 1949)
34. Y.H. Shih, C.O. Alley, Phys. Rev. Lett. **61**, 2921 (1988)
35. S. Magnitskiy, D. Frolovtsev, V. Firsov, P. Gostev, I. Protsenko, M. Saygin, J. Russ. Laser Res. **36**, 618 (2015)
36. S. Friberg, C.K. Hong, L. Mandel, Phys. Rev. Lett. **54**, 2011 (1985)
37. F.J. Duarte, T.S. Taylor, *Quantum Entanglement Engineering and Applications* (Institute of Physics, Bristol, 2021)
38. R. Menzel, A. Heuer, D. Puhlmann, K. Dechoum, M. Hillery, M.J.A. Spähn, W.P. Schleich, J. Mod. Opt. **60**, 86–94 (2013)
39. E. Bolduc, J. Leach, F.M. Miatto, G. Leuchs, R.W. Boyd, PNAS **111**, 12337–12341 (2014)
40. A.S.D. Sandanayaka, T. Matsushima, F. Bencheikh, S. Terakawa, W.J. Potscavage, C. Qin, T. Fujihara, K. Goushi, J.-C. Ribierre, C. Adachi, Appl. Phys. Express **12**, 061010 (2019)
41. I.W.D. Samuel, G.A. Turnbull, Chem. Rev. **107**, 1272 (2007)
42. G. Xie, M. Chen, M. Mazilu, S. Zhang, A.K. Bansal, K. Dhokalia, I.D.W. Samuel, Laser Photonics Rev. **10**, 82 (2016)